Environmental Science and Pollution Research (2022) 29:4431–4445
https://doi.org/10.1007/s11356-021-15970-4

RESEARCH ARTICLE

Adsorption of estrone, 17β-estradiol, and 17α-ethinylestradiol from water onto modified multi-walled carbon nanotubes, carbon cryogel, and carbonized hydrothermal carbon

Danijela Prokić[1] · Marija Vukčević[2] · Angelina Mitrović[3] · Marina Maletić[1] · Ana Kalijadis[4] · Ivona Janković-Častvan[2] · Tatjana Đurkić[2]

Received: 20 April 2021 / Accepted: 10 August 2021 / Published online: 18 August 2021

Abstract

Carbon materials of different structural and textural properties (multi-walled carbon nanotubes, carbon cryogel, and carbonized hydrothermal carbon) were used as adsorbents for the removal of estrone, 17β-estradiol, and 17α-ethinylestradiol from aqueous solutions. Chemical modification and/or activation were applied to alter surface characteristics and to increase the adsorption and desorption efficiency of carbon materials. Surfaces of treated and untreated carbon materials were characterized through the examination of the textural properties, the nature of surface functional groups, and surface acidity. It was found that the adsorption capacity of tested carbon materials is not directly proportional to the specific surface area and the content of surface oxygen groups. However, a high ratio of surface mesoporosity affected the adsorption process most prominently, by increasing adsorption capacity and the rate of the adsorption process. Adsorption of estrone, 17β-estradiol, and 17α-ethinylestradiol followed pseudo-second-order kinetic model, while the equilibrium adsorption data were best fitted with the Langmuir isotherm model. Calculated mean adsorption energy values, along with the thermodynamic parameters, indicated that removal of selected hormones was dominated by the physisorption mechanism. High values of adsorption efficiency (88–100 %) and Langmuir adsorption capacities (29.45–194.7 mg/g) imply that examined materials, especially mesoporous carbon cryogel and multi-walled carbon nanotubes, can be used as powerful adsorbents for relatively fast removal of estrogen hormones from water.

Keywords Carbon cryogel · Multi-walled carbon nanotubes · Hydrothermal carbon · Surface modification · Adsorption · Estrogenic hormones

Introduction

Hormones, both naturally secreted or of synthetic origin, are trace pollutants of major concerns due to their potential of disrupting the endocrine activities of living organisms (Auriol et al. 2006). Steroid estrogens are attracting great attention because of their high estrogenic potential. Although present at very low concentrations (the order of magnitude ng/L) (Auriol et al. 2008), these compounds still can cause serious adverse effects on aquatic organisms (Snyder et al. 2004) and domestic animals (Gao et al. 2019). Many pathological phenomena, such as carcinogenicity, disorders in reproductive function, and decreased fertility in fish, are induced by the presence of steroid estrogens in the environment (Vilela et al. 2018; Khanal et al. 2006; Bilal and Iqbal 2019). The principal way in which these compounds reach the environment is through municipal wastewater. These hormones are not removed from sewage in wastewater treatment plants completely, so their effluents contain a significant concentration of these substances (Vilela et al. 2018). These substances may also pose a risk to humans and animals indirectly, via food contamination (Hartmann et al. 1998). In this regard, the

Responsible editor: Tito Roberto Cadaval Jr

✉ Danijela Prokić
dprokic@tmf.bg.ac.rs

[1] Innovation Center of the Faculty of Technology and Metallurgy, Karnegijeva 4, Belgrade 11000, Serbia

[2] Faculty of Technology and Metallurgy, University of Belgrade, Karnegijeva 4, Belgrade 11000, Serbia

[3] Institute for Technology of Nuclear and Other Mineral Raw Materials, Bulevar Franše d'Eperea 86, Belgrade 11000, Serbia

[4] Department of Materials "VINČA" Institute of Nuclear Sciences - National Institute of the Republic of Serbia, University of Belgrade, Mike Petrovica Alasa 12-14, Belgrade 11000, Serbia

removal of estrogens from water has become a very important issue worldwide.

Different methods for removing estrogens from water have been used so far, such as adsorption (Wang et al. 2018; Tagliavini et al. 2017), membrane filtration (Akanyeti et al. 2017; Tagliavini and Schäfer 2018), biodegradation (Fernández et al. 2017), advanced oxidation process (Fonseca et al. 2011), and photodegradation (Sornalingam et al. 2016; Zhang et al. 2007). Adsorption is considered one of the most efficient and economical processes, and the choice of appropriate adsorbent is the key element in the application of this method (Tang et al. 2018; Wang et al. 2018). Different materials were used so far as adsorbents for the removal of steroid estrogens from water such as chitin, chitosan, activated carbon (Zhang and Zhou 2005; Tagliavini et al. 2017), hybrid clay materials (Thanhmingliana et al. 2016), magnetic graphene oxide (Wang et al. 2018), cyclodextrin polymers (Tang et al. 2018), and iron nanoparticles (Ali et al. 2017).

Carbon materials gained increasing attention as highly efficient adsorbents for both organic and inorganic substances from the aqueous phase due to their specific surface characteristics, which can easily be tailored or modified (Lalović et al. 2017; Ren et al. 2011). Different types of carbon materials, such as activated carbon (Tagliavini et al. 2017), carbon nanotubes (Kumar and Mohan 2012), pyrolyzed coke (Gökce and Arayici 2016), activated charcoal (Kumar and Mohan 2011), bone chare (Patel et al. 2015), reduced graphene oxide-magnetic composite (Luo et al. 2017), and magnetic biochar nanoparticles (Dong et al. 2018), were used for estrogen adsorption from water so far. In our previous work (Prokić et al. 2020), it was shown that activated carbon cloth modified with HNO_3 demonstrated high efficiency in removal of estrone (E1), 17β-estradiol (E2), and 17α-ethinylestradiol (EE2) from water.

This paper aimed to examine the efficiency of different carbon materials for adsorption and desorption of estrone, 17β-estradiol, and 17α-ethinylestradiol and to reveal which features of material surface affect the adsorption process most prominently. Therefore, carbon materials of different structural and textural properties (carbonized hydrothermal carbon, carbon cryogel, and multi-walled carbon nanotubes) were chosen, while activation or chemical modification was applied to access the influence of surface chemistry on the adsorption process. Material selection was made based on their specific characteristics. The highly porous and hollow structure of multi-walled carbon nanotubes (MWCNTs), as well as developed and controllable porosity of carbon cryogels (CCs), provides strong interaction between material surface and adsorbate molecules. Additionally, the mainly mesoporous structure of these materials allows a fast transfer of adsorbate molecules through the pore network (Celzard et al. 2012; Minović et al. 2015). Due to these textural characteristics, MWCNTs are proven to be a good adsorbent for hormones removal (Dai et al. 2019). Consequently, it is reasonable to expect equally high efficiency of CCs in hormone removal, although, to the best of our knowledge, CCs were not used for hormones removal so far. Following the recent trend in producing carbon materials from different types of biomass waste (Falco et al. 2011), carbonized hydrothermal carbon (CHTC) and activated carbonized hydrothermal carbon (ACHTC), produced from waste beach sawdust, was applied for the first time as an adsorbent for estrone, 17β-estradiol, and 17α-ethinylestradiol removal from water. The process of hormone adsorption onto selected materials was studied by examining the influence of temperature, contact time, and initial concentration of hormone solution. Based on experimental data, adsorption kinetics was investigated and compared with theoretical models, while the equilibrium data were analyzed with Langmuir, Freundlich, Dubinin-Radushkevich, and Temkin isotherms.

Experimental

Material preparation

MWNCTs with an average external diameter of 6–9 nm and a length of 5 μm were purchased from Sigma-Aldrich, USA. CC was manufactured in the Institute of Nuclear Science Vinča, National Institute of the Republic of Serbia. CC was obtained by pyrolyzing resorcinol-formaldehyde cryogel in an inert atmosphere (Minović et al. 2015). CHTC and ACHTC were prepared by carbonization and activation of sawdust-based hydrothermal carbon. The hydrothermal synthesis was carried out in an autoclave, at a temperature of 180 °C, under self-generated pressure, for 24 h. The reaction mixture consisted from 6 g of sawdust, 400 mL distilled water, and 0.015 g citric acid (which was used as a catalyst). The solid product obtained by hydrothermal synthesis was filtered and washed with methanol and distilled water. Hydrothermal carbon was carbonized in an inert nitrogen atmosphere, up to a temperature of 900 °C, at a heating rate of 5 °C/min to obtain sample CHTC. Sample ACHTC was obtained by activation of CHTC using KOH as an activating agent. The mass ratio of KOH and CHTC was 2/1. According to the literature (Lalović et al. 2017; Vukčević et al. 2013; Carvajal-Bernal et al. 2015; Sajjadi et al. 2019), chemical modification, using HNO_3, HCl, and KOH, can alter the surface chemistry of different carbon materials, increasing their adsorption capacity. Therefore, chemical modification of MWCNTs and CCs was performed as it was described in the literature (Lalović et al. 2017): samples modify with HNO_3 (MWCNT/HNO_3 and CC/HNO_3) and KOH (MWCNT/KOH and CC/KOH) were obtained by heating at 80 °C MWCNTs and CCs in 4 M HNO_3 and 4 M KOH solution, respectively, for 4h; samples modify with HCl (MWCNT/HCl and CC/HCl) were obtained by submerging

unmodified materials in 1 M HCl for 4 h at room temperature. After chemical treatments, modified samples were thoroughly washed with distilled water to neutral pH and dried at 110 °C for 24 h. Applied treatment conditions are summarized in Table 1.

Sample characterization

Surface and porosity analyzer Micromeritics ASAP 2020 (Micromeritics Instrument Corporation, USA) was used to obtain nitrogen adsorption-desorption isotherms and to examine textural characteristics of carbon samples. The micropore volume (V_{micro}), specific surface area (S_{BET}), and microporous surface area (S_{micro}) were determined from the adsorption data using the manufacturer's software ASAP 2020 V3.05 H. External surface area, including mesoporous area (S_{meso}), is gained by subtracting of S_{micro} from S_{BET}. Pore size distribution was estimated according to Barrett, Joyner, and Halenda (BJH) method (Barrett et al. 1951).

The pH values of aqueous slurries (pH slurry) of the examined materials were measured as follows: 0.2 g of each material was immersed in 2 mL of deionized water. The samples were stored in a plastic tube, under N_2, at room temperature. pH values of the samples were measured after reaching the equilibrium.

Determination of functional groups, present on the surface of examined carbon materials, was performed by Fourier transform infrared spectroscopy (FTIR). FTIR spectra were recorded in the range from 400 to 4000 cm^{-1} by applying Bomem MB-Series spectrometer (Hartmann & Braun).

Hormone adsorption on different carbon materials

The adsorption efficiency of examined materials was investigated in a batch system with constant mixing (200 rpm). Carbon materials (0.02 g) were immersed in a 25 mL hormone solution. The initial pH of the solution was adjusted to 7, using diluted CH_3COOH and NH_4OH solution. After adsorption, all samples were filtered through the PVDF 0.45 μm filters. The concentration of tested hormones was analyzed by liquid chromatography-tandem mass spectrometry (LC-MS/MS).

Adsorption kinetics

Experiments of adsorption kinetics were conducted on all tested materials in order to identify the adsorption rate and to test the effect of time on the adsorption process. A solution of hormone mixture (containing E1, E2, and EE2), with an initial concentration of 5 mg/L for each hormone, was prepared. All materials were immersed in 25 mL of the solution. The samples were taken after 3, 5, 10, 15, 30, 60, 120, 180 min, and 24 h of adsorption. For the calculation of adsorption kinetic parameters, the following kinetic models were applied, pseudo-first-order model (Equation 1) (Lagergren 1898; Yu et al. 2020; Cai et al. 2019), pseudo-second-order model (Equation 2) (Ho and McKay 1999; Cai et al. 2019), Elovich model (Equation 3) (Weber and Morris 1963), and intra-particle diffusion model (Equation 4) (Aharoni and Ungarish 1976), that are expressed as:

$$q_t = q_e \cdot \left(1 - e^{-k_1 t}\right) \tag{1}$$

$$q_t = q_e - \left(\frac{1}{q_e} + k_2 \cdot t\right)^{-1} \tag{2}$$

$$q_t = \frac{1}{\beta}\ln(\alpha \cdot \beta) + \frac{1}{\beta}\ln t \tag{3}$$

$$q_t = k_{id} \cdot t^{\frac{1}{2}} + C \tag{4}$$

where q_e (mg/g) is the amount of adsorbed hormone per unit mass of the adsorbent at equilibrium; q_t (mg/g) is the amount of adsorbed hormone per unit mass of the adsorbent at time t; k_1 is the first-order adsorption rate constant (min^{-1}); k_2 is the second-order adsorption rate constant (g/mg min); k_{id} (mg/g $min^{1/2}$) is the intra-particle diffusion rate constant that can be evaluated from the slope of the linear plot of q_t versus $t^{1/2}$, and constant C is the intercept; Elovich constant α (g/mg min) is related to the initial adsorption rate, and β (g/mg) is a

Table 1 Applied conditions for carbon adsorbent preparation

Carbon material	Treatment conditions
MWCNT	-
MWCNT/HNO_3	Chemical modification: 4M HNO_3, 4 h, 80°C
MWCNT/HCl	Chemical modification: 1M HCl, 4 h, room temperature
MWCNT/KOH	Chemical modification: 4M KOH, 4 h, 80°C
CC	-
CC/HNO_3	Chemical modification: 4M HNO_3, 4 h, 80°C
CC/KOH	Chemical modification: 4M KOH, 4 h, 80°C
CHTC	Carbonization: 900 °C, 5 °C/min, N_2 atmosphere
ACHTC	Activation: KOH:CHTC = 2:1, 900 °C, 5 °C/min, N_2 atmosphere

constant related to the extent of surface coverage and activation energy for chemisorption.

Adsorption isotherms

The adsorption isotherm studies were carried out at an initial hormone solution concentration of 2, 4, 6, 8, 10, 12, 25, and 50 mg/L. Taking into account adsorption efficiency based on the results of the previous experiment, the materials MWCNT/KOH, CC/KOH, and ACHTC were chosen as adsorbents. The samples were taken after 24 h of adsorption. The equilibrium experimental data were fitted by using the Langmuir (Langmuir 1918) and Freundlich (Freundlich 1906) isotherm models. These two isotherm models are expressed as Equations (5) and (6), respectively:

$$q_e = \frac{Q_0 \cdot b \cdot C_e}{1 + b \cdot C_e} \tag{5}$$

$$q = K_f \cdot C_e^{1/n} \tag{6}$$

where C_e is the equilibrium hormone concentration (mg/L), q_e is the amount of adsorbed hormone per unit weight of the adsorbent at equilibrium (mg/g), Q_0 is the maximum adsorption capacity (mg/g), b is the Langmuir isotherm constant, and K_f and n are the Freundlich constant and heterogeneity factor, respectively.

In order to examine whether the adsorption process is of the physical or chemical nature, experimental data were fitted by Dubinin-Radushkevich (D-R) isotherm (Inyinbor et al. 2016), given by the following equation:

$$\ln q_e = \ln q_m - \beta\varepsilon^2 \tag{7}$$

where q_m is the monolayer sorption capacity (mg/g), β is the activity coefficient related to sorption energy (mol^2 J^{-2}), and ε is the Polanyi potential, expressed in Equation (8):

$$\varepsilon = RT\ln\left(1 + \frac{1}{C_e}\right) \tag{8}$$

where R is gas constant (kJ/mol K) and T is the absolute temperature (K).

The mean adsorption energy, E (kJ/mol), is given by Equation (9):

$$E = (-2\beta)^{-1/2} \tag{9}$$

The Temkin adsorption isotherm can be expressed by the following equation (Inyinbor et al. 2016):

$$q_e = B\ln A + B\ln C_e \tag{10}$$

where $B = RT/b$, b is the Temkin constant related to the heat of sorption (J/mol), and A is the Temkin isotherm constant (L/g).

Thermodynamic studies

The effect that surrounding temperature has on adsorption capacities of MWCNT/KOH, CC/KOH and ACHTC was studied in batch, temperature-controlled system, at temperatures of 25, 35, 45, and 55 °C: 0.02 g of selected carbon material was immersed in 25 mL of E1, E2, and EE2 aqueous solution (initial concentration of each hormone was 5 mg/L) and constantly shaken for 3 h. The thermodynamics of adsorption process were estimated using the following equations (Ifelebuegu 2012)

$$\ln K_c = \frac{\Delta S^0}{R} - \frac{\Delta H^0}{RT} \tag{11}$$

$$\Delta G^0 = \Delta H^0 - T\Delta S^0 \tag{12}$$

Thermodynamic parameters ΔH^0 and ΔS^0 were estimated from the slopes and intercepts of $\ln K_c$ vs. $1/T$ plots, while value of ΔG^0 was calculated following Equation (12).

Adsorption of hormones from real water samples

Real water samples of groundwater, surface water, and wastewater were spiked with a mixture of E1, E2, and EE2 solution to obtain an initial concentration of 5 mg/dm^3 each hormone in water samples. Water samples were collected from Belgrade Ranney wells (groundwater), river Pek (surface water), and from the entrance to the water purification plant Aranđelovac (wastewater). Adsorption of hormones from spiked water samples (25 mL) was performed onto 0.02 g of carbon material (MWCNT/KOH, CC/KOH, and ACHTC) in the batch system with constant shaking at room temperature.

Desorption experiments

Desorption of hormones from materials was performed using dichloromethane/methanol (1:1, v/v) mixture in a flow system. Five milliliters of the solvent mixture was loaded through the column containing examined carbon adsorbent. Prior to the solvent elution, carbon packing was left to soak for 10 min. The obtained eluent was evaporated to the dryness under nitrogen and reconstituted in 25 mL of the mobile phase, which consisted of 75% methanol and 25% formic acid (0.1% water solution).

LC-MS/MS analysis

Separation of selected hormones was done using a Surveyor LC system (Thermo Fisher Scientific, USA). The reverse-

phase separation was conducted using an Agilent Zorbax Eclipse XDB-C18 analytical column (75 mm × 4.6 mm × 3.5 μm). The mobile phase composition was 25 % formic acid (0.1 % water solution) and 75 % methanol at a constant flow rate of 0.3 mL/min. The method was isocratic. LCQ Advantage (Thermo Fisher Scientific, USA) mass spectrometer with electrospray ion source and quadrupole ion trap mass analyzer was used for detection and quantification of the hormones. The measurements were recorded in the positive ionization mode.

Results and discussion

Material characterization

Nitrogen adsorption and desorption isotherms for unmodified samples, multi-walled carbon nanotubes, carbon cryogel, and carbonized hydrothermal carbon, are presented in Fig. 1a, as the function of the adsorbed amount of N_2, and relative pressure at −196 °C. According to the IUPAC classification (Sing et al. 1985), isotherms of MWCNT and CC are of type IV with an H_2-hysteresis loop. These are characteristics for the pores of undefined shape on the mesoporous materials. Isotherms of CHTC are of type I, related to the microporous materials. At high P/P_0, adsorption, isotherm obtained for CHTC does not exhibit any limiting adsorption, which is related to the non-rigid aggregates of plate-like particles and slit-shaped pores (Lowell et al. 2004). Pore size distribution (PSD) of MWCNT, CC, and CHTC is shown in Fig. 1b. Wide PSD, obtained for MWCNT and CC, with an average diameter of 14.98 and 12.14 nm, respectively, confirmed the mesoporous character of these materials. On the other hand, PSD of sample CHTC is very narrow, with an average pore diameter of 1.5 nm, which is characteristic of microporous materials.

The textural characteristics of all, unmodified and modified materials, along with the pH slurry values are summarized in Table 2. Activated carbon material, ACHTC, exhibited the highest specific surface area. From the results obtained for CHTC and ACHTC, it can be observed that activation of CHTC led to a drastic increase in specific surface area from 213 to 1002 m^2/g, remaining the microporous character of the surface, with the slight increase in mean pore diameter from 1.5 to 2.9 nm. Applied chemical treatments did not have a significant influence on the specific surface area of MWCNT, since S_{BET} of modified MWCNTs differs less than 10 %, compared with the unmodified sample. On the other hand, chemical modification more considerably affects the specific surface area of carbon cryogel, decreasing the S_{BET} from 10.8 % (CC/KOH) to 18.42 % (CC/HNO_3). Also, a slight increase in mean pore diameter was observed for modified MWCNTs and CCs, along with the changes in micropore volume and mesoporous surface.

Results given in Table 2 reveal that there are high variations between pH slurry values of the examined materials. These values range from mildly acidic (4.71 of material ACHTC) to basic (9.68 of unmodified CC). Applied chemical treatments altered the surface acidity of tested materials. As it can be seen from pH slurry values, modification with HNO_3 and HCl increased surface acidity, while modification with KOH decreased surface acidity of carbon nanotubes and, unexpectedly, increased the surface acidity of CC.

FTIR spectra of all examined materials are presented in Fig. 2. All spectra exhibit a broad absorption band at approximately 3435 cm^{-1}, which can be attributed to the stretching vibration of OH groups (Biniak et al. 1997), and this peak is the most pronounced in the spectra of CC/HNO_3. Two small peaks in the region 2850–2950 cm^{-1}, present in FTIR spectra of all tested samples, can be assigned to symmetrical and asymmetrical vibrations of C-H in methyl or methylene groups (Lazić et al. 2018). The broad band around 1630 cm^{-1} at MWCNTs spectra and two poorly separated bands at 1620 and 1640 cm^{-1} at CCs, CHTC, and ACHTC spectra can be assigned to the vibrations of the aromatic C=C bond and the bending vibration of the O-H bond, or the stretching vibration of the aliphatic C=C bond (Maletić et al. 2019; Chen et al. 2012; Sevilla and Fuertes 2009; Kalijadis et al. 2015; Rusmirović et al. 2018). The bands observed around 1383

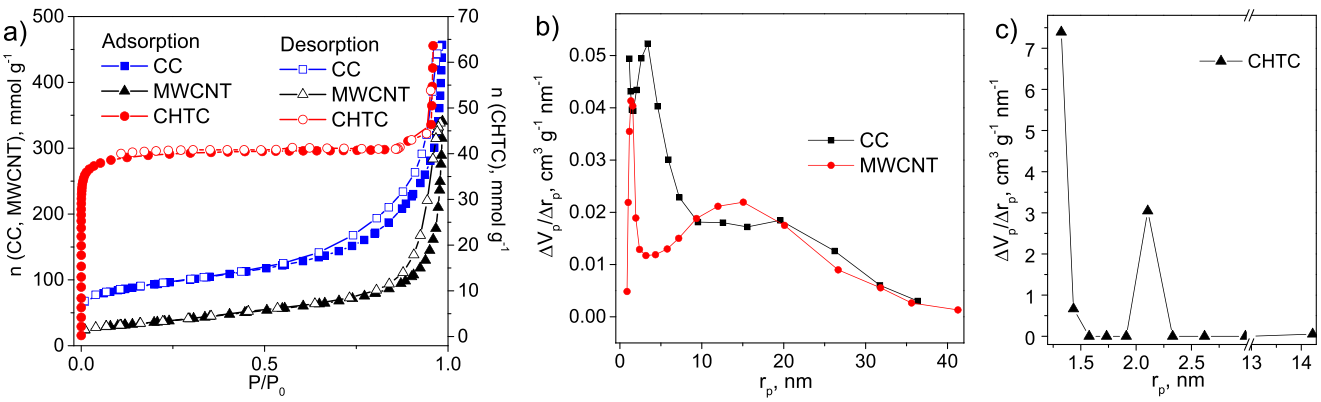

Fig. 1 Nitrogen adsorption isotherms (**a**) and pore size distribution for unmodified MWCNT and CC (**b**) and CHTC (**c**)

Table 2 Textural characteristics and pH slurry of examined materials

Materials	S_{BET}, m^2/g	S_{micro}, m^2/g	S_{meso}, m^2/g	S_{meso}/S_{micro}	V_{micro}, cm^3/g	D_{mean}, nm	pH slurry
MWCNT	252	16.3	235.8	14.47	0.0749	14.98	6.06
MWCNT/HNO_3	258	10.0	248.1	24.81	0.0761	18.14	4.25
MWCNT/KOH	246	9.8	236.1	24.09	0.0719	17.88	8.24
MWCNT/HCl	239	7.3	231.2	31.67	0.0692	17.16	5.96
CC	612	226.1	385.9	1.71	0.2347	12.14	9.68
CC/HNO_3	499	163.1	336.1	2.06	0.1891	13.14	5.07
CC/KOH	546	155.5	390.6	2.51	0.2075	15.38	5.44
CHTC	213	210	3	0.01	0.187	1.5	7.53
ACHTC	1002	947	55	0.06	0.479	2.9	4.71

cm^{-1} for all samples can be attributed to the O-H bond in the carboxyl group (Barroso-Bogeat et al. 2014; Rusmirović et al. 2018). The bands observed in the region 1360–1000 cm^{-1} correspond to C-O stretching and OH banding vibration (Sevilla and Fuertes 2009). The absorption bands in the region below 800 cm^{-1} probably correspond to out-of-plane bending vibration of C-H groups located at the edges of aromatic planes (Biniak et al. 1997; Goreacioc 2015).

Although there are no significant differences in the types of surface functionalities, induced by applied chemical treatments, observed differences in the peak intensity imply the alteration in content of surface oxygen groups. Most pronounced changes are visible in the spectra of MWCNTs due to a decrease in intensity of bands located in the region 1300–1000 cm^{-1} after modification. Changes in this region can be related to the decreased amount of hydroxyl, ester, or ether groups. A decrease in intensity of peaks around 2850–2950 cm^{-1} observed after HNO_3 and HCl modification of MWCNT and after activation of CHTC implicates that some of the aliphatic groups were oxidized during the treatments (Prokić et al. 2020). It can be noticed that chemical modification of CC leads to an increase in the intensity of the peaks in 1360–1000 cm^{-1} region, which is more pronounced for HNO_3-treated sample. The spectrum of CC/HNO_3 also displays the low-intensity shoulder peak at 1730 cm^{-1} which corresponds to C=O stretching vibration in carboxyl groups (Zhang et al. 2015). Applied chemical treatment with HNO_3, as well as activation, brought a significant increase in the intensity of carboxylic C=O peak at 1383 cm^{-1} for CC/HNO_3, MWCNT/HNO_3, and ACHTC samples, while the peak at 670 cm^{-1} was most prominently increased in the spectra of MWCNT/KOH and ACHTC. An increased amount of carboxyl groups, observed in the FTIR spectra of CC/HNO_3, MWCNT/HNO_3, and ACHTC (Fig. 2), is consistent with the increased acidity of these samples (Table 2).

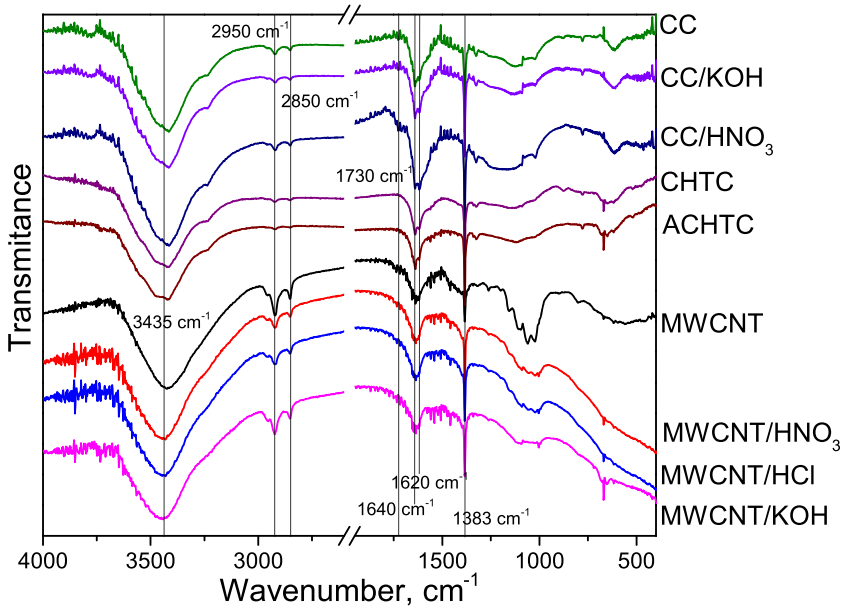

Fig. 2 FTIR spectra of examined carbon materials

Adsorption and desorption efficiency

The efficiency of examined materials to adsorb E1, E2, and EE2 from water is presented in Fig. 3a. Most of the examined materials almost completely remove estrogen hormones from water, with adsorption efficiency ranging from 87.22 to 99.76 %, the only exception being CHTC with an efficiency of around 50 % for all hormones. Low adsorption efficiency of sample CHTC is the most likely a consequence of low specific surface area. Also, the predominant microporosity of sample CHTC may hinder the diffusion of large hormone molecules and consequently reduce their adsorption. However, the activation of CHTC strongly improved the adsorption efficiency up to 98.2 %. The highest adsorption efficiency, ranging from 99.20 % for E2 to 99.54 % for EE2, was observed for unmodified MWCNT, the material with moderate S_{BET} value implying that the efficiency is not directly proportional to the specific surface area.

The highest desorption efficiency (Fig. 3b), from 91.27 % for E2 to 99.81 % for EE2, was gained for sample MWCNT/KOH, while the lowest results were obtained for CHTC (34.51 % for E2 – 46.23 % for E1). It can be observed that applied activation slightly increased desorption efficiency, since sample ACHTC showed higher desorption efficiency than CHTC. The increase in the ratio of mesoporosity and pore diameter of sample ACHTC enabled easier hormone diffusion during both adsorption and desorption process. In the case of CC samples, modification has negative or no influence on desorption efficiency, while modification of MWCNTs led to the largest differences in desorption

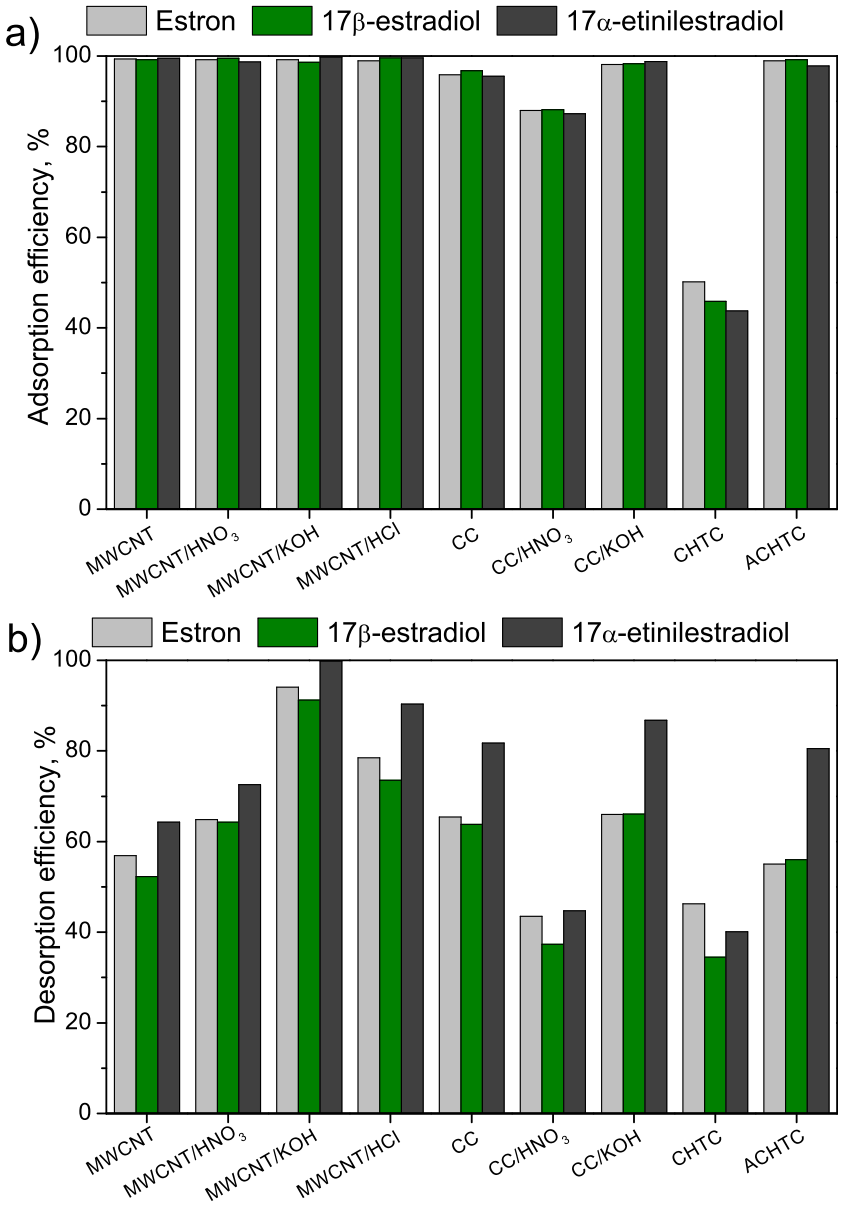

Fig. 3 Adsorption (**a**) and desorption (**b**) efficiency of examined materials toward estrogen hormones

efficiency. Changes in the MWCNTs surface chemistry, induced by applied modifications, most likely affected the adsorption mechanism by favoring physisorption, which led to the easier desorption of hormones from the adsorbent surface.

Adsorption kinetics

The influences of contact time on E1, E2, and EE2 adsorption onto different carbon materials are presented in Fig. 4. MWCNT samples exhibited the highest adsorption capacities and fast adsorption process, which reached its equilibrium in approximately 30–60 min. CC samples also showed good adsorption capacities in a somewhat slower adsorption process, since the materials were saturated after 180 min. Although CHTC showed the fastest adsorption, reaching the equilibrium in less than 30 min, its adsorption capacity was the lowest.

In order to investigate the kinetics of hormone adsorption onto examined carbon materials, experimental data were fitted with pseudo-first-order and pseudo-second-order kinetic models (Fig. 4), Elovich model (Figure S1), and intra-particle diffusion model (Figure S2).

All tested hormones showed similar adsorption behavior. Kinetic parameters for estrone adsorption, obtained by fitting the experimental data with different kinetic models, along with the experimentally obtained equilibrium amounts of estrone ($q_{e,\,exp}$) are summarized in Table 3, while kinetic parameters for adsorption of 17β-estradiol and 17α-ethinylestradiol are shown in Supplementary Material, Table S1 and S2. Results revealed that all tested samples, except CHTC, showed high adsorption capacities toward examined hormones in the range from 5.34 to 6.16 mg/g.

According to the values of correlation coefficients (R^2) obtained for pseudo-first and pseudo-second model kinetics, experimental data for almost all tested samples fits better with pseudo-second model kinetics, which suggests that the chemisorption may be the rate-limiting step in the process of hormone adsorption on tested materials (Mita et al. 2017). However, the somewhat different finding was obtained by comparing the values of $q_{e\ exp}$ and $q_{e\ cal}$, obtained by these kinetic models: although no clear relationship was observed between the type of material and the applied kinetic model, it was noticed that adsorption of hormones onto mesoporous materials (MWCNT and CC) oxidized with HNO_3 particularly follows the pseudo-second-order kinetic. On the other hand, adsorption of hormones onto CC and MWCNT treated with KOH preferably follows the pseudo-first-order model. Although lower values of correlation coefficients obtained for the Elovich model (Fig. S1) indicate that this model does not describe hormone adsorption well enough, it was observed that applied chemical modification and activation led to differences in surface coverage (β) and initial rate of adsorption (α). The values of rate constants (k_1 and k_2) indicate that the adsorption process was faster on materials that have a higher ratio of mesoporosity (S_{meso}/S_{micro}, Table 2). Also, the value of Elovich constant α is higher for materials having higher S_{meso}/S_{micro}. The fastest adsorption was observed on MWCNTs, which have the highest ratio of mesoporosity, and the estrogen hormones easily access the porous material structure. On the other hand, microporous materials are characterized by slower adsorption, due to the hindered hormone diffusion through the micropores. Taking into consideration surface characteristics of examined materials (Table 2) and values of $q_{e,\,exp}$ (Tables 3, S1, and S2), it can be observed that neither surface acidity nor specific surface area has a decisive influence on the adsorption kinetics of tested materials.

To examine the mechanism of hormone adsorption onto tested materials, and to reveal which process influences the rate of adsorption, intra-particle diffusion model was used. Multi-linearity in the intra-particle diffusion plots (Fig. S2), obtained for all tested materials, except CHTC, suggests that the rate of hormone adsorption onto tested carbon materials could be affected by the intra-particle diffusion, since hormone adsorption occurs through the three stages (Table 3, Tables S1 and S2): fast surface adsorption, moderate intra-particle diffusion stage, and the final slow equilibrium stage,

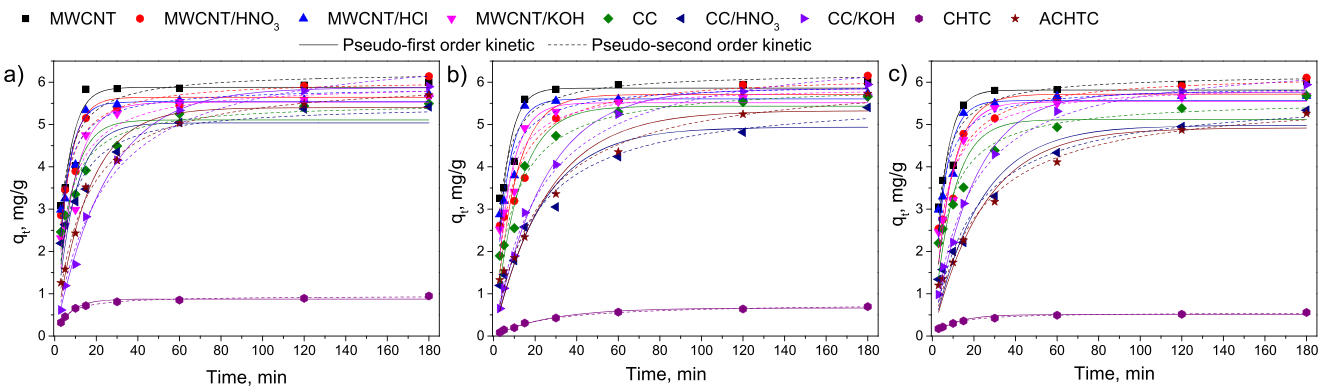

Fig. 4 Kinetic data obtained for **a** E1, **b** E2, and **c** EE2 adsorption onto different carbon materials fitted with pseudo-first and pseudo-second-order kinetic model

Table 3 Kinetic parameters and correlation coefficients for adsorption of E1 onto different carbon materials

Material	MWCNT	MWCNT/ HNO_3	MWCNT/ HCl	MWCNT/ KOH	CC	CC/ HNO_3	CC/ KOH	CHTC	ACHTC
$q_{e\ exp}$, mg/g	5.99	6.14	5.72	5.64	5.49	5.42	5.89	0.95	5.69
Pseudo-first order									
R^2	0.85922	0.84849	0.89108	0.90328	0.80147	0.81767	0.99607	0.95914	0.9712
k_1, min^{-1}	0.181	0.172	0.186	0.114	0.135	0.112	0.0404	0.137	0.0625
$q_{e\ cal}$, mg/g	5.88	5.64	5.54	5.53	5.11	5.04	5.87	0.87	5.40
Pseudo-second order									
R^2	0.87939	0.94497	0.92507	0.91835	0.94949	0.94923	0.98443	0.98818	0.99177
k_2, g/mg min	0.291	0.261	0.299	0.167	0.196	0.160	0.043	0.190	0.0757
$q_{e\ cal}$, mg/g	6.25	6.06	5.89	5.98	5.53	5.48	6.93	0.95	6.11
Elovich model									
R^2	0.60914	0.76472	0.69382	0.74112	0.88935	0.82036	0.82736	0.68592	0.87504
α, mg/g min	316.77	102.51	229.47	16.56	19.05	15.35	1.035	0.14	19.16
β, g/mg	1.95	1.79	1.99	1.51	1.61	1.66	0.97	2.77	1.13
Intra-particle diffusion									
R_1^2	0.82408	0.9047	0.91894	0.7557	0.97136	0.98928	0.98049	0.95774	0.93794
$k_{id,1}$, mg/g $min^{1/2}$	1.195	0.986	1.075	1.048	0.546	0.558	0.950	0.071	0.820
C_1, mg/g	0.822	1.127	0.947	0.279	1.613	1.325	1.036	0.286	0.115
R_2^2	0.90184	0.94233	0.84004	0.85769	0.64372	0.81182	0.84202	-	0.96127
$k_{id,2}$, mg/g $min^{1/2}$	0.017	0.103	0.027	0.197	0.164	0.180	0.101	-	0.119
C_2, mg/g	5.753	4.750	5.329	4.053	3.735	3.471	4.588	-	4.133
R_3^2	0.93167	1	1	0.99924	1	1	1	-	1
$k_{id,3}$, mg/g $min^{1/2}$	0.010	0.0005	0.013	0.017	0.019	0	0.006	-	0.017
C_3, mg/g	5.808	6.135	5.541	5.403	5.240	5.417	5.814	-	5.464

which involves adsorption and desorption within the particle and on the external surface. The fact that none of the stages in the multi-linear intra-particle diffusion plots passes through the origin suggests that the intra-particle diffusion is not the only rate-controlling step in the overall adsorption process. On the other hand, experimental data obtained for CHTC were fitted with one straight line passing near to the origin (intercepts ranged from 0.014 mg/g for EE2 to 0.286 mg/g for E1). This indicates that adsorption of E1, E2, and EE2 onto CHTC is controlled by intra-particle diffusion due to a very low ratio of mesoporosity and specific surface area.

Adsorption isotherms

One of each type of material (multi-walled carbon nanotubes, carbon cryogel, and carbonized hydrothermal carbon) was selected for adsorption isotherms study and to examine the influence of initial hormone concentration on adsorption. MWCNT/KOH, CC/KOH, and ACHTC were selected as samples with high adsorption and the highest desorption efficiency (Fig. 3). The equilibrium data for adsorption of tested hormones onto MWCNT/KOH, CC/KOH, and ACHTC fitted with the Langmuir and the Freundlich isotherm models are shown in Fig. 5, while fitting with Temkin (Fig. S3) and Dubinin-Radushkevich (Fig. S4) isotherm models are shown in Supplementary Material.

Adsorption capacities of examined materials increase with initial hormones concentration, although the characteristic plateau was not reached in the examined concentration range, especially in the case of MWCNT/KOH and CC/KOH. The calculated parameters of model fittings are given in Table 4. According to R^2, the Langmuir model is most suitable for describing the equilibrium hormone adsorption, although equilibrium data can be well fitted with Freundlich and Temkin isotherm models, also. This indicates that adsorption of the hormones on the surface of MWCNT/KOH, CC/KOH, and ACHTC occurs mostly homogeneously, with no interaction between adsorption molecules (Luo et al. 2017) and that adsorption includes uniform distribution of binding energies. Obtained maximum adsorption capacities, calculated from the Langmuir isotherm model, were high for all examined hormones, ranging from 29.45 to 194.7 mg/g (Table 4), and the highest value of Q_0 was obtained for E2 adsorption onto CC/KOH. The mean adsorption energy, E, obtained by Dubinin-Radushkevich model ranged from 3.774 kJ/mol, for adsorption of E1 onto CC/KOH, to 5.774 kJ/mol for adsorption of

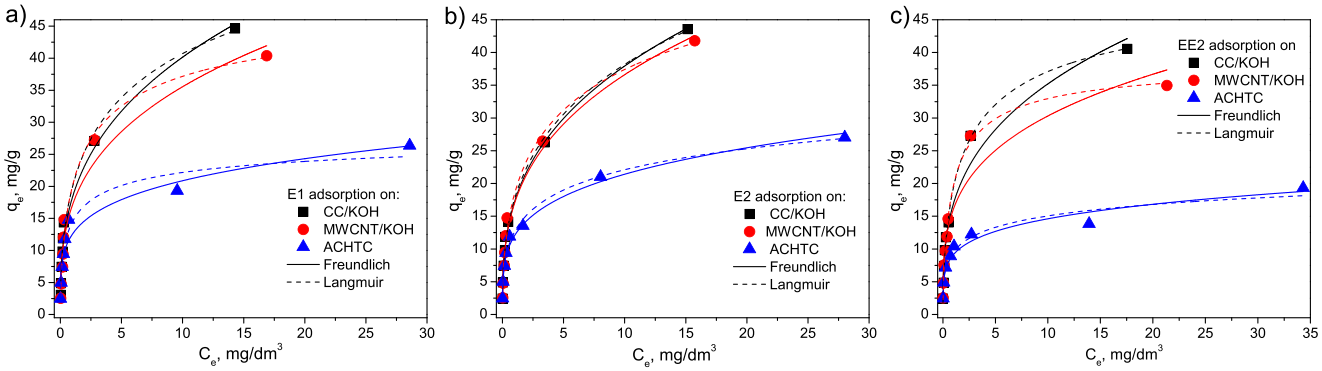

Fig. 5 Equilibrium data of **a** E1, **b** E2, and **c** EE2 adsorption onto CC/KOH, MWCNT/KOH, and ACHTC fitted with Freundlich and Langmuir isotherm models

EE2 onto ACHTC, while Temkin constant B, related to the heat of adsorption, ranged from 2.023 J/mol for EE2 adsorption onto ACHTC to 6.909 J/mol for E1 adsorption onto CC/KOH. These results suggest that adsorption of E1, E2, and EE2 onto examined carbon materials occur through the mechanism of physisorption.

Comparison of values of maximum adsorption capacities of the present and some previous studies is given in Table 5. Based on the results presented in Table 5, it can be concluded that values of Q_0 obtained in the present study are comparable or higher than those presented in the literature. Therefore, examined materials, especially MWCNT/KOH and CC/KOH, can be used as highly efficient adsorbents for the removal of estrogen hormones from water.

Thermodynamic studies

Thermodynamic studies of E1, E2, and EE2 adsorption on MWCNT/KOH, CC/KOH, and ACHTC were performed at four different temperatures (25, 35, 45, and 55 °C) to gain insight into the mechanism by which examined hormones were adsorbed onto the tested materials.

Generally, the adsorption capacities of tested carbon samples increase with the temperature (Fig. 6). For mesoporous samples (MWCNT/KOH and CC/KOH), only a slight increase in adsorption capacities was observed, while microporous sample (ACHTC) showed the highest increase in adsorption capacity by increasing temperature from 25 to 35 °C. The increase in temperature enabled facilitated diffusion of hormone molecules through the porous matrices of examined

Table 4 Isotherm parameters for adsorption of E1, E2, and EE2 onto MWCNT/KOH, CC/KOH, and ACHTC

Material	MWCNT/KOH			CC/KOH			ACHTC		
Hormone	E1	E2	EE2	E1	E2	EE2	E1	E2	EE2
Langmuir adsorption isotherm									
R^2	0.98639	0.99038	0.99292	0.98505	0.99559	0.99653	0.95144	0.99153	0.95210
Q_0, mg/g	50.55	74.31	39.22	83.78	194.7	52.90	29.45	51.09	30.75
b	0.663	0.331	1.002	0.314	0.100	0.576	0.972	0.329	0.450
Freundlich adsorption isotherm									
R^2	0.95719	0.98333	0.91730	0.98031	0.99547	0.96793	0.93676	0.98475	0.95112
K_f, $mg^{1-1/n}L^{1/n}g^{-1}$	17.15	17 .04	16.09	18.38	17.26	16.90	12.58	12.06	9.14
$1/n$	0.316	0.332	0.275	0.034	0.342	0.319	0.220	0.249	0.204
Temkin adsorption isotherm									
R^2	0.963	0.9486	0.9656	0.9774	0.8023	0.9254	0.9623	0.9648	0.9599
A, l/g	35.584	38.517	46.730	29.702	0.134	44.114	127.224	87.379	155.28
B, J/mol	5.959	5.865	5.016	6.909	4.478	5.506	2.989	3.176	2.023
Dubinin-Radushkevich adsorption isotherm									
R^2	0.8335	0.8306	0.8717	0.8829	0.8368	0.7477	0.8337	0.8414	0.8411
q_m mg/g	63.158	69.258	70.66	50.36	79.92	79.74	105.438	96.68	109.456
E, kJ/mol	4.385	4.564	4.499	3.774	4.891	5.157	5.624	5.621	5.774

Table 5 Comparison of maximum adsorption capacities, calculated from Langmuir isotherm model, of different materials as adsorbents for E1, E2, and EE2

Hormone	Adsorbent	$C_{adsorbate}$, mg/L	$C_{sorbent}$, g/L	Q_0, mg/g	Ref
E1 E2	Rice husk	3–12	4	2.698 1.649	Honorio et al. (2018)
E2	Bone chare	5 and 9	0.5–50	10.12	Patel et al. (2015)
E1 E2	Zeolite/HDTMA	2–20	1	25.58 13.004	Zhong et al. (2019)
E2	MWCNTs/FMBO	0.2–6	0.05	47.25	Dai et al. (2019)
EE2	MWCNT	0.025–0.1	0.5	5.59×10^{-3}	Kumar and Mohan (2012)
EE2	MWCNT	10–200	1	15.5	Silva et al. (2020)
E2	MWCNT-C/$C_oF_{e2}O_4$ MWCNT-N/$C_oF_{e2}O_4$	0.4–2.4	0.1	29.1 31.8	Wang et al. (2015)
EE2	MWCNT	5–70	0.2	26	Teixeira et al. (2013)
E1 E2	Pyrolyzed coke	0.1×10^{-3}–1×10^{-3}	0.025–0.25	0.05 0.033	Gökce and Arayici (2016)
E2	Activated charcoal Activated charcoal supported titanate nanotubes	0.1–1.5	0.5	2.57 2.78	Huang et al. (2020)
E1 E2	ACC	2–12	0.8	12.34 12.66	Prokić et al. (2020)
EE2				11.11	
E1 E2	MWCNT/KOH	2–50	0.8	50.55 74.31	This study
EE2				39.22	
E1	CC/KOH			83.78	
E2				194.7	
EE2				52.90	
E1	ACHTC			29.45	
E2				51.09	
EE2				30.75	

carbon materials, and more favorable adsorption, which is especially noticeable for sample ACHTC.

The thermodynamic parameters, calculated from Equations (11) and (12), are summarized in Table 6.

According to the obtained ΔH and ΔG values, adsorption of E1, E2, and EE2 onto MWCNT/KOH, CC/KOH, and ACHTC is spontaneous endothermic process, favorable at the higher temperatures. The values of Gibbs free energy, ranging from −15.93 to −6.62 kJ/mol (Table 5), imply that tested estrogen hormones were adsorbed onto MWCNT/KOH, CC/KOH, and ACHTC through the mechanism of physisorption, which is in agreement with the results obtained by adsorption isotherms studies. Enthalpy values obtained for hormone adsorption on MWCNT/KOH and CC/KOH also suggest that adsorption occurs through the mechanism of physisorption, while the enthalpy values obtained for hormone adsorption on ACHTC, falling in the range from 60 to 82 kJ/mol, suggest a rather chemical nature of the adsorption process. The positive entropy values from 66 to 299 J/mol K suggest increased randomness after the adsorption process (Ifelebuegu 2012)

Adsorption of hormones from real water samples

Adsorption of E1, E2, and EE2 from spiked samples of surface water, groundwater, and wastewater was performed in order to assess the selectivity of MWCNT/KOH, CC/KOH, and ACHTC toward hormones. The results were compared to the results obtained from spiked samples of deionized water to examine the matrix effect of real water samples, i.e., presence of other pollutants, on adsorption capacities of these materials. Only slight changes in adsorption capacities (lower than 10 %) were observed, compared to the adsorption from deionized water (Fig. 7). These results suggest that the matrix of real water samples does not affect the adsorption capacities of MWCNT/KOH, CC/KOH, and ACHTC significantly, which showed high selectivity towards examined hormones.

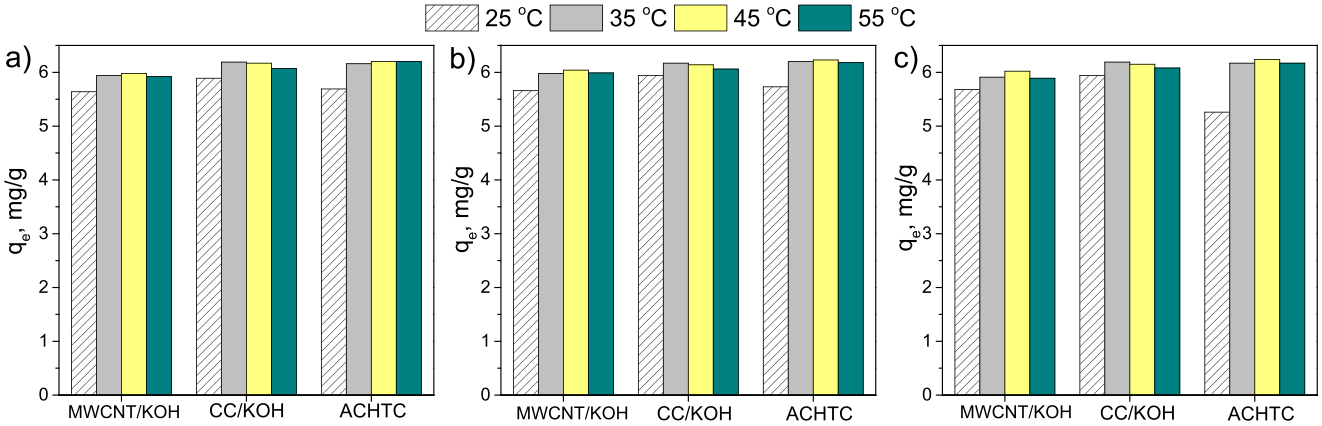

Fig. 6 Effect of temperature on **a** E1, **b** E2, and **c** EE2 adsorption on MWCNT/KOH, CC/KOH, and ACHTC

Table 6 Thermodynamic parameters for adsorption of E1, E2, and EE2 onto MWCNT/KOH, CC/KOH, and ACHTC

Thermodynamic parameters	T	MWCNT/KOH			CC/KOH			ACHTC		
		E1	E2	EE2	E1	E2	EE2	E1	E2	EE2
ΔH^0, kJ/mol		17.79	23.63	16.37	17.34	10.35	12.37	69.83	60.00	82.07
ΔS^0, kJ/molK		0.082	0.102	0.078	0.089	0.066	0.073	0.259	0.230	0.299
ΔG^0, kJ/mol	298.15	−6.62	−6.79	−6.75	−9.25	−9.20	−9.42	−7.49	−8.59	−6.97
	308.15	−7.44	−7.81	−7.53	−10.15	−9.86	−10.15	−10.08	−10.89	−9.95
	318.15	−8.26	−8.83	−8.30	−11.04	−10.52	−10.88	−12.67	−13.19	−12.94
	328.15	−9.08	−9.85	−9.08	−11.93	−11.17	−11.61	−15.27	−15.49	−15.93

Conclusions

Chemical modification and activation were applied on different carbon materials to alter their surface characteristics and increase their efficiency in the adsorption and desorption of estrone, 17β-estradiol, and 17α-ethinylestradiol. Applied chemical treatments led to an increase in pore diameter, followed by changes in microporous and mesoporous surface, while activation in the presence of KOH increased specific surface area almost five times. On the other hand, the content of surface oxygen groups was not considerably affected by applied treatments. It was found that the adsorption capacities of examined carbon materials are not directly proportional to the specific surface area and the content of surface oxygen groups. However, a high ratio of mesoporosity was proved to be the crucial factor for the increase in adsorption capacity

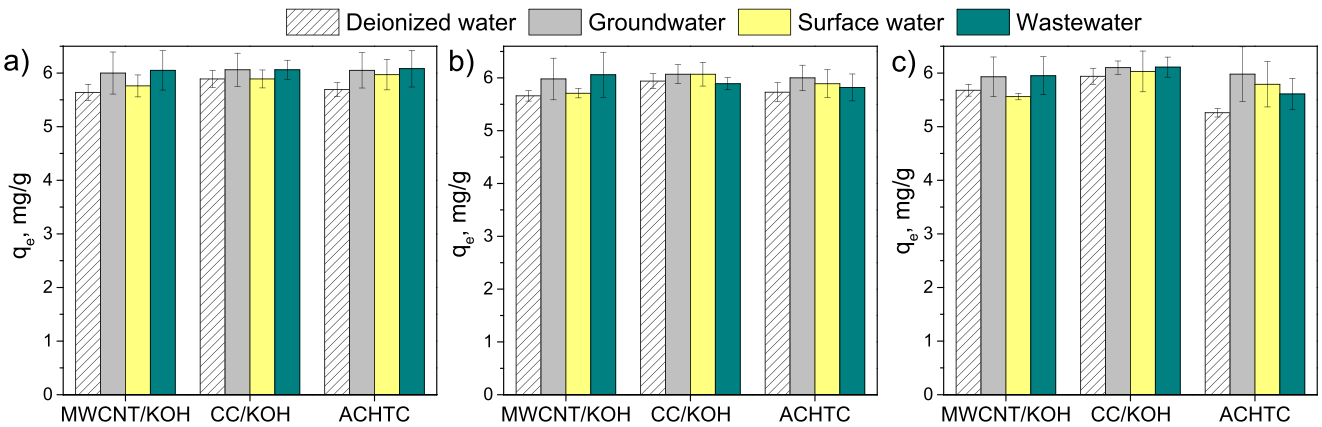

Fig. 7 Influence of real water sample matrices on **a** E1, **b** E2, and **c** EE2 adsorption on MWCNT/KOH, CC/KOH, and ACHTC

and the rate of the adsorption process, due to facilitated hormone diffusion to the adsorption sites. The adsorption process can be described by pseudo-second-order kinetics model, and equilibrium data showed a slightly better agreement with Langmuir adsorption isotherm. The mean adsorption energy values and thermodynamic parameters showed that adsorption of estrone, 17β-estradiol, and 17α-ethinylestradiol was a spontaneous and endothermic process, dominated by the physisorption mechanism. High adsorption capacities, and selectivity toward estrone, 17β-estradiol, and 17α-ethinylestradiol, imply that examined materials, especially mesoporous multi-walled carbon nanotubes and carbon cryogel, can be used as adsorbents for the removal of estrogen hormones from water.

Supplementary Information The online version contains supplementary material available at https://doi.org/10.1007/s11356-021-15970-4.

Author contribution Conceptualization, Tatjana Đurkić; material preparation and investigation, Danijela Prokić, Angelina Mitrović, Ana Kalijadis, and Ivona Janković-Častvan; data analysis and writing-original draft, Marina Maletić and Danijela Prokić; and writing-review and editing the paper, Marija Vukčević and Tatjana Đurkić. All authors read and approved the final manuscript.

Funding The research was funded by the Ministry of Education, Science and Technological Development of the Republic of Serbia (Contract No. 451-03-9/2021-14/200135 and Contract No. 451-03-9/2021-14/200287).

Data availability Data sharing is not applicable to this article as no datasets were generated or analyzed during the current study.

Declarations

Ethics approval and consent to participate Not applicable.

Consent for publication Not applicable.

Competing interests The authors declare no competing interests.

References

Aharoni C, Ungarish M (1976) Kinetics of activated chemisorption. Part 1.—The non-elovichian part of the isotherm. J Chem Soc Faraday Trans 1(72):265–268. https://doi.org/10.1039/F19767200400

Akanyeti I, Kraft A, Ferrari CH (2017) Hybrid polystyrene nanoparticle-ultrafiltration system for hormone removal from water. J Water Process Eng 17:102–109. https://doi.org/10.1016/j.jwpe.2017.02.014

Ali I, Alothman ZA, Alwarthan A (2017) Supra molecular mechanism of the removal of 17-β-estradiol endocrine disturbing pollutant from water on functionalized iron nano particles. J Mol Liq 241:123–129. https://doi.org/10.1016/j.molliq.2017.06.005

Auriol M, Meknassi Y, Tyagi RD, Adams CD, Surampalli RY (2006) Endocrine disrupting compounds removal from wastewater, a new challenge. Process Biochem 41:525–539. https://doi.org/10.1016/j.procbio.2005.09.017

Auriol M, Filali-Meknassi Y, Craig DA, Tyagi RD, Noguerol TN, Piña B (2008) Removal of estrogenic activity of natural and synthetic hormones from a municipal wastewater: efficiency of horseradish peroxidase and laccase from Trametes versicolor. Chemosphere 70:445–452. https://doi.org/10.1016/j.chemosphere.2007.06.064

Barrett EP, Joyner LD, Halenda PP (1951) The determination of pore volume and area distributions in porous substances. I. Computations from nitrogen isotherms. J Am Chem Soc 73:373–380. https://doi.org/10.1021/ja01145a126

Barroso-Bogeat A, Alexandre-Franco M, Fernández-González C, Gómez-Serrano V (2014) FT-IR analysis of ayrone and chromene structures in activated carbon. Energy Fuel 28:4096–4103. https://doi.org/10.1021/ef5004733

Bilal M, Iqbal HMN (2019) Persistence and impact of steroidal estrogens on the environment and their laccase-assisted removal. Sci Total Environ 690:447–459. https://doi.org/10.1016/j.scitotenv.2019.07.025

Biniak S, Szymański G, Siedlewski J, Świą-tkowski A (1997) The characterization of activated carbons with oxygen and nitrogen surface groups. Carbon 35:1799–1810. https://doi.org/10.1016/S0008-6223(97)00096-1

Cai Y, Liu L, Tian H, Zhennai Y, Luo X (2019) Adsorption and desorption performance and mechanism of tetracycline hydrochloride by activated carbon-based adsorbents derived from sugar cane bagasse activated with $ZnCl_2$. Molecules 24:4534. https://doi.org/10.3390/molecules24244534

Carvajal-Bernal AM, Gomez F, Giraldo L, Moreno-Pirajan JC (2015) Adsorption of phenol and 2,4-dinitrophenol on activated carbons with surface modifications. Microporous Mesoporous Mater 209:150–156. https://doi.org/10.1016/j.micromeso.2015.01.052

Celzard A, Fierro V, Amaral-Labat G (2012) Adsorption by carbon gels. In: Tascón JMD (ed) Novel Carbon Adsorbents. Elsevier, Oxford, pp 207–244. https://doi.org/10.1016/B978-0-08-097744-7.00007-7

Chen CM, Zhang Q, Yang MG, Huang CH, Yang YG, Wang MZ (2012) Structural evolution during annealing of thermally reduced graphene nanosheets for application in supercapacitors. Carbon 50:3572–3584. https://doi.org/10.1016/j.carbon.2012.03.029

Dai MY, Liu YG, Zeng GM, Liu SB, Ning QM (2019) Adsorption studies of 17β-estradiol from aqueous solution using a novel stabilized Fe–Mn binary oxide nanocomposite. Environ Sci Pollut Res 26:7614–7626. https://doi.org/10.1007/s11356-019-04173-7

Dong X, He L, Hu H, Liu N, Gao S, Piao Y (2018) Removal of 17β-estradiol by using highly adsorptive magnetic biochar nanoparticles from aqueous solution. Chem Eng J 352:371–379. https://doi.org/10.1016/j.cej.2018.07.025

Falco C, Baccile N, Titirici MM (2011) Morphological and structural differences between glucose, cellulose and lignocellulosic biomass derived hydrothermal carbons. Green Chem 13:3273–3281. https://doi.org/10.1039/c1gc15742f

Fernández L, Louvado A, Esteves VI, Gomes NCM, Almeida A, Cunha Â (2017) Biodegradation of 17β-estradiol by bacteria isolated from deep sea sediments in aerobic and anaerobic media. J Hazard Mater 323:359–366. https://doi.org/10.1016/j.jhazmat.2016.05.029

Fonseca AP, Lima DLD, Esteves VI (2011) Degradation by solar radiation of estrogenic hormones monitored by UV-Visible spectroscopy and capillary electrophoresis. Water Air Soil Pollut 215:441–447. https://doi.org/10.1007/s11270-010-0489-7

Freundlich HMF (1906) Adsorption in Solution. Phys Chem 57:384–410

Gao P, Liang Z, Zhao Z, Wang W, Yang C, Hu B, Cui F (2019) Enhanced adsorption of steroid estrogens by one-pot synthesized phenyl-modified mesoporous silica: dependence on phenyl-organosilane precursors and pH condition. Chemosphere 234:438–449. https://doi.org/10.1016/j.chemosphere.2019.06.089

Gökce CE, Arayici S (2016) Adsorption of 17β-estradiol and estrone by activated carbon derived from sewage sludge. Desalin Water Treat 57:2503–2514. https://doi.org/10.1080/19443994.2015.1034183

Goreacioc T (2015) Oxidation and characterization of active carbon AG-5. Chem J Mold 10:76–83. https://doi.org/10.19261/cjm.2015.10(1).11

Hartmann S, Lacorn M, Steinhart H (1998) Natural occurrence of steroid hormones in food. Food Chem 62:7–20. https://doi.org/10.1016/S0308-8146(97)00150-7

Ho YS, McKay G (1999) Pseudo-second order model for sorption processes. Process Biochem 34:451–465. https://doi.org/10.1016/S0032-9592(98)00112-5

Honorio JF, Veit MT, Suzaki PYR, Coldebella PF, Sloboda Rigobello E, Tavares CRG (2018) Adsorption of naturals hormones estrone, 17β-estradiol and estriol by rice husk: monocomponent and multicomponent kinetics and equilibrium. Environ Technol 41:1075–1092. https://doi.org/10.1080/09593330.2018.1521472

Huang T, Pan B, Ji H, Liu W (2020) Removal of 17β-estradiol by activated charcoal supported titanate nanotubes (TNTs@AC) through initial adsorption and subsequent photo-degradation: Intermediates, DFT calculation, and mechanisms. Water 12:2121. https://doi.org/10.3390/w12082121

Ifelebuegu AO (2012) Removal of steroid hormones by activated carbon adsorption—kinetic and thermodynamic studies. J Environ Prot 3:469–475. https://doi.org/10.4236/jep.2012.36057

Inyinbor AA, Adekola FA, Olatunji GA (2016) Kinetics, isotherms and thermodynamic modeling of liquid phase adsorption of rhodamine B dye onto Raphia hookerie fruit epicarp. Water Resour Ind 15:14–27. https://doi.org/10.1016/j.wri.2016.06.001

Kalijadis A, Đorđević J, Trtić-Petrović T, Vukčević M, Popović M, Maksimović V, Rakočević Z, Laušević Z (2015) Preparation of boron-doped hydrothermal carbon from glucose for carbon paste electrode. Carbon 95:42–50. https://doi.org/10.1016/j.carbon.2015.08.016

Khanal SK, Xie B, Thompson ML, Sung S, Ong SK, Van Leeuwen J (2006) Fate, transport, and biodegradation of natural estrogens in the environment and engineered systems. Environ Sci Technol 40:6537–6546. https://doi.org/10.1021/es0607739

Kumar AK, Mohan SV (2011) Endocrine disruptive synthetic estrogen (17α-ethynylestradiol) removal from aqueous phase through batch and column sorption studies: mechanistic and kinetic analysis. Desalination 276:66–74. https://doi.org/10.1016/j.desal.2011.03.022

Kumar AK, Mohan SV (2012) Removal of natural and synthetic endocrine disrupting estrogens by multi-walled carbon nanotubes (MWCNT) as adsorbent: kinetic and mechanistic evaluation. Sep Purif Technol 87:22–30. https://doi.org/10.1016/j.seppur.2011.11.015

Lagergren S (1898) Zur theorieder sogennanten adsorption geloester stoffe. Bih till K Sven Vetenskapsakademiens, Handl 24:1–39

Lalović B, Đurkić T, Vuković M, Janković-Častvan I, Kalijadis A, Laušević Z, Laušević M (2017) Solid-phase extraction of multiclass pharmaceuticals from environmental water samples onto modified multi-walled carbon nanotubes followed by LC-MS/MS. Environ Sci Pollut Res 24:20784–20793. https://doi.org/10.1007/s11356-017-9748-0

Langmuir I (1918) The adsorption of gases on plane surfaces of glass, mica and platinum. J Am Chem Soc 40:1361–1403

Lazić BD, Pejić BM, Kramar AD, Vukčević MM, Mihajlovski KR, Rusmirović JD, Kostić MM (2018) Influence of hemicelluloses and lignin content on structure and sorption properties of flax fibers (Linum usitatissimum L.). Cellulose 25:697–709. https://doi.org/10.1007/s10570-017-1575-4

Lowell S, Shields JE, Thomas MA, Thommes M (2004) Characterization of porous solids and powders: surface area, pore size and density. Springer, Dordrecht

Luo Z, Li H, Yang Y, Lin H, Yang Z (2017) Adsorption of 17α-ethinylestradiol from aqueous solution onto a reduced graphene oxide-magnetic composite. J Taiwan Inst Chem Eng 80:797–804. https://doi.org/10.1016/j.jtice.2017.09.028

Maletić M, Vukčević M, Kalijadis A, Janković-Častvan I, Dapčević A, Laušević Z, Laušević M (2019) Hydrothermal synthesis of TiO_2/carbon composites and their application for removal of organic pollutants. Arab J Chem 12:4388–4397. https://doi.org/10.1016/j.arabjc.2016.06.020

Minović TZ, Gulicovski JJ, Stoiljkovic MM, Jokic BM, Živković LS, Matovic BZ, Babić BM (2015) Surface characterization of mesoporous carbon cryogel and its application in arsenic (III) adsorption from aqueous solutions. Microporous Mesoporous Mater 201:271–276. https://doi.org/10.1016/j.micromeso.2014.09.031

Mita L, Forte M, Rossi A, Adamo C, Rossi S, Mita DG, Guida M, Portaccio M, Godievargova T, Yavour I, Samir M, Eldin M (2017) Removal of 17-α Ethinylestradiol from water systems by adsorption on polyacrylonitrile beads: isotherm and kinetics studies. Peertechz J Environ Sci Toxicol 2:48–58. https://doi.org/10.17352/pjest.000012

Patel S, Han J, Gao W (2015) Sorption of 17β-estradiol from aqueous solutions on to bone char derived from waste cattle bones: kinetics and isotherms. J Envron Chem Eng 3:1562–1569. https://doi.org/10.1016/j.jece.2015.04.027

Prokić D, Vukčević M, Kalijadis A, Maletić M, Babić B, Đurkić T (2020) Removal of estrone, 17β-estradiol, and 17α-ethinylestradiol from water by adsorption onto chemically modified activated carbon cloths. Fibers Polym 21:2263–2274. https://doi.org/10.1007/s12221-020-9758-2

Ren X, Chen C, Nagatsu M, Wang X (2011) Carbon nanotubes as adsorbents in environmental pollution management: a review. Chem Eng J 170:395–410. https://doi.org/10.1016/j.cej.2010.08.045

Rusmirović JD, Rančić MP, Pavlović VB, Rakić VM, Stevanović S, Đonlagić J, Marinković AD (2018) Cross-linkable modified nanocellulose/polyester resin-based composites: effect of unsaturated fatty acid nanocellulose modification on material performances. Macromol Mater Eng 303:1700648. https://doi.org/10.1002/mame.201700648

Sajjadi B, Zubatiuk T, Leszczynska D, Leszczynski J, Chen WY (2019) Chemical activation of biochar for energy and environmental applications: a comprehensive review. Rev Chem Eng 35:777–815. https://doi.org/10.1515/revce-2018-0003

Sevilla M, Fuertes AB (2009) The production of carbon materials by hydrothermal carbonization of cellulose. Carbon 47:2281–2289. https://doi.org/10.1016/j.carbon.2009.04.026

Silva RCF, Ardisson JD, Chaves Cotta AA, Araujo MH, Carvalho Teixeira AP (2020) Use of iron mining tailings from dams for carbon nanotubes synthesis in fluidized bed for 17α-ethinylestradiol removal. Environ Pollut 260:114099. https://doi.org/10.1016/j.envpol.2020.114099

Sing KSW, Everett DH, Haul RAW, Moscou L, Pierotti RA, Rouquerol J, Siemieniewska T (1985) Reporting physisorption data for gas/solid systems with special reference to the determination of surface area and porosity. Pure Appl Chem 57:603–619. https://doi.org/10.1351/pac198557040603

Snyder SA, Westerhoff P, Yoon Y, Sedlak DL (2004) Pharmaceuticals, personal care products, and endocrine disruptors in water: implications for the water industry. Environ Eng Sci 20:449–469. https://doi.org/10.1089/109287503768335931

Sornalingam K, McDonagh A, Zhou JL (2016) Photodegradation of estrogenic endocrine disrupting steroidal hormones in aqueous systems : progress and future challenges. Sci Total Environ 550:209–224. https://doi.org/10.1016/j.scitotenv.2016.01.086

Tagliavini M, Schäfer AI (2018) Removal of steroid micropollutants by polymer-based spherical activated carbon (PBSAC) assisted membrane Filtration. J Hazard Mater 353:514–521. https://doi.org/10.1016/j.jhazmat.2018.03.032

Tagliavini M, Engel F, Weidler PG, Scherer T, Schäfer AI (2017) Adsorption of steroid micropollutants on polymer-based spherical activated carbon (PBSAC). J Hazard Mater 337:126–137. https://doi.org/10.1016/j.jhazmat.2017.03.036

Tang P, Sun Q, Suo Z, Zhao L, Yang H, Xiong X, Pu H, Gan N, Li H (2018) Rapid and efficient removal of estrogenic pollutants from water by using beta- and gamma-cyclodextrin polymers. Chem Eng J 344:514–523. https://doi.org/10.1016/j.cej.2018.03.127

Teixeira APC, Purceno AD, de Paula CCA, da Silva JCC, Ardisson JD, Lago RM (2013) Efficient and versatile fibrous adsorbent based on magnetic amphiphilic composites of chrysotile/carbon nanostructures for the removal of ethynilestradiol. J Hazard Mater 248–249: 295–302. https://doi.org/10.1016/j.jhazmat.2013.01.014

Thanhmingliana LC, Tiwari D, Lee SM (2016) Efficient removal of 17β-estradiol using hybrid clay materials: batch and column studies. Environ Eng Res 21:203–210. https://doi.org/10.4491/eer.2016.003

Vilela CLS, Bassin JP, Peixoto RS (2018) Water contamination by endocrine disruptors: Impacts, microbiological aspects and trends for environmental protection. Environ Pollut 235:546–559. https://doi.org/10.1016/j.envpol.2017.12.098

Vukčević M, Kalijadis A, Babić B, Laušević Z, Laušević M (2013) Influence of different carbon monolith preparation parameters on pesticide adsorption. J Serb Chem Soc 78:1617–1632. https://doi.org/10.2298/JSC131227006V

Wang F, Sun W, Pan W, Xu N (2015) Adsorption of sulfamethoxazole and 17β-estradiol by carbon nanotubes/CoFe2O4 composites. Chem Eng J 274:17–29. https://doi.org/10.1016/j.cej.2015.03.113

Wang X, Liu Z, Ying Z, Huo M, Yang W (2018) Adsorption of trace estrogens in ultrapure and wastewater treatment plant effluent by magnetic graphene oxide. Int J Environ Res Public Health 15: 1454. https://doi.org/10.3390/ijerph15071454

Weber WJ, Morris JC (1963) Kinetics of adsorption on carbon from solutions. J Sanit Eng Div Am Soc Civil Eng 89:31–59

Yu Z, Hu C, Dichiara AB, Jiang W, Gu J (2020) Cellulose nanofibril/carbon nanomaterial hybrid aerogels for adsorption removal of cationic and anionic organic dyes. Nanomaterials 10:169. https://doi.org/10.3390/nano10010169

Zhang Y, Zhou JL (2005) Removal of estrone and 17β-estradiol from water by adsorption. Water Res 39:3991–4003. https://doi.org/10.1016/j.watres.2005.07.019

Zhang Y, Zhou JL, Ning B (2007) Photodegradation of estrone and 17β-estradiol in water. Water Res 41:19–26. https://doi.org/10.1016/j.watres.2006.09.020

Zhang H, Ming R, Yang G, Li Y, Li Q, Shao H (2015) Influence of alkali treatment on flax fiber for use as reinforcements in polylactide stereocomplex composites. Polym Eng Sci 55:2553–2558. https://doi.org/10.1002/pen.24147

Zhong S, Zhang S, Zhang Y, Li C (2019) Performance and mechanism of estrone (E1) and 17β-estradiol (17β-E2) removal from aqueous solution using hexadecyltrimethylammonium (HDTMA) modified zeolites. J Mater Sci Mater Electron 30:20410–20419. https://doi.org/10.1007/s10854-019-02375-w